

Receptor-Based Virtual Ligand Screening for the Identification of Novel CDC25 Phosphatase Inhibitors

Matthieu Montes,^{†,‡,§} Emmanuelle Braud,^{†,‡,§} Maria A. Miteva,^{‡,§} Mary-Lorène Goddard,^{‡,§}
Odile Mondésert,^{||} Stéphanie Kolb,^{‡,§} Marie-Priscille Brun,^{‡,§} Bernard Ducommun,^{||}
Christiane Garbay,^{‡,§} and Bruno O. Villoutreix^{*,‡,§}

UFR biomédicale, Laboratoire de Pharmacochimie Moléculaire et Cellulaire, Université Paris Descartes,
Paris, F-75006, France, INSERM U648, Paris, F-75006, France, and CNRS, UMR 5088-IFR 109,
University of Toulouse, Route de Narbonne, 31062 Toulouse, France

Received August 20, 2007

CDC25 phosphatases play critical roles in cell cycle regulation and are attractive targets for anticancer therapies. Several small non-peptide molecules are known to inhibit CDC25, but many of them appear to form a covalent bond with the enzyme or act through oxidation of the thiolate group of the catalytic cysteine. Structure-based virtual ligand screening computations were performed with FRED, Surflex, and LigandFit, a compound collection of over 310 000 druglike molecules and the crystal structure of CDC25B in order to identify novel classes of ligands. In vitro experiments carried out on a selected list of 1500 molecules led to the discovery of 99 compounds able to inhibit CDC25B activity at 100 μ M. Further docking computations were applied, allowing us to propose a binding mode for the most potent molecule ($IC_{50} = 13 \mu$ M). Our best compounds represent promising new classes of CDC25 inhibitors that also exhibit antiproliferative properties.

INTRODUCTION

CDC25 dual-specificity phosphatases are key activators of the cell cycle progression.¹ They catalyze the dephosphorylation of two adjacent phosphothreonine and phosphotyrosine residues of the cyclin-dependent kinases (Cdk/cyclins) subunit and thus activate the Cdk/cyclin complexes, allowing for the initiation and progression of the cell cycle.² Three isoforms have been identified in human cells, namely CDC25A, CDC25B, and CDC25C.^{3–5} Among them, CDC25B seems to play an essential role in the G2/M phase as a mitotic starter by activating the Cdk1/cyclinB complex.⁶ The CDC25s share with other PTPases the consensus His-Cys(X)₅-Arg (X being any residue) signature, while the three-dimensional (3D) structures of these two protein classes differ significantly.^{7,8} Overproduction of both CDC25A and CDC25B correlates with a wide variety of tumors of high impact. For instance, CDC25B overexpression has been observed in breast,⁹ colorectal,¹⁰ head and neck,¹¹ or nonsmall cell lung cancer patients.^{12,13} As such, small molecules inhibiting the activity of CDC25 and more specifically of CDC25B may afford new approaches to the treatment of cancer.¹⁴

Over the past few years, several synthetic and natural molecules with different structural features targeting CDC25 activity have been reported.^{15–18} These inhibitors usually have IC_{50} values in the micromolar range (from 1 to 90 μ M), except for a few quinone derivatives like NSC663284¹⁹ or BN82685²⁰ that show IC_{50} values in the high nanomolar range. The small non-peptide inhibitors of CDC25 belong

to diverse chemical classes including vitamin K₃ and its derivatives, quinolinediones, and naphthoquinones (reviewed in ref 14). However, many of these molecules contain reactive groups and can, for example, covalently modify the active site cysteine residue through sulfhydryl arylation or could form an ether linkage with serine residues, suggesting that novel inhibitors lacking such reactive groups would be very valuable to assist in the development of new antineoplastic agents.

In the present study, we aimed at the development of new inhibitors (e.g., new scaffolds) of CDC25B. Since the 3D structure of this protein is known,⁸ it is possible to apply in silico structure-based virtual ligand screening (SB-VLS) technologies to search for new CDC25 inhibitors.^{21,22} We decided to perform a multistep SB-VLS experiment using an ADME/Tox-filtered compound collection containing over 310 000 unique molecules and three different docking/scoring packages. These computations were followed by diverse in vitro experiments and further redocking. Application of our in silico/in vitro procedure allowed us to identify several promising inhibitors of CDC25. To the best of our knowledge, it is the first report that applies SB-VLS experiments to the CDC25 target.

EXPERIMENTAL METHODS

Target Preparation and Binding Site Definition. The crystal structure of CDC25B was retrieved from the Protein Data Bank²³ (PDB code 1CWT⁸). All heteroatoms were removed from the file, and hydrogen atoms were added using the program InsightII. Correct charge assignment in the protein binding pocket can be important, thus we performed pK_a predictions using our Protein Continuum Electrostatic server^{24,25} for all potentially ionizable groups (i.e., Arg, Lys,

* Corresponding author fax: +33142862065; e-mail: bruno.villoutreix@univ-paris5.fr.

[†] These authors contributed equally to the manuscript.

[‡] Université Paris Descartes.

[§] INSERM U648.

^{||} University of Toulouse.

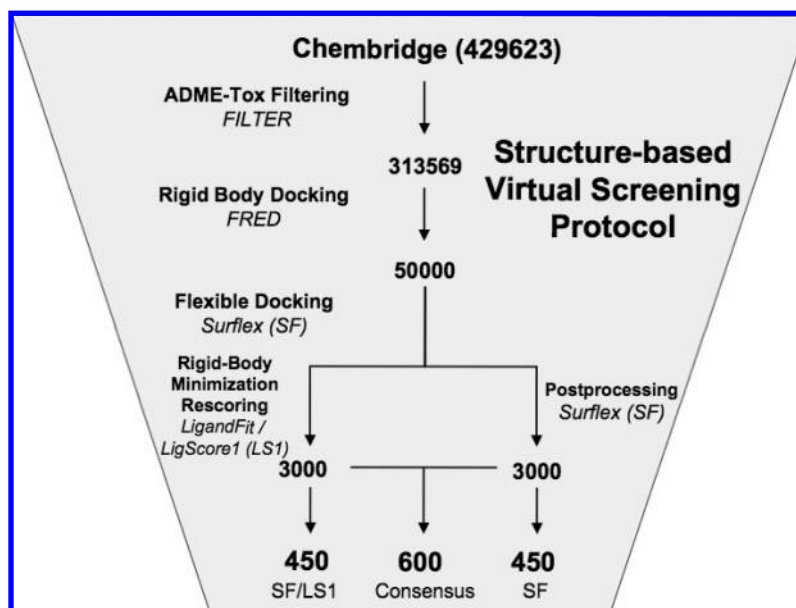


Figure 1. SB-VLS strategy. SF/LS1: compounds after Surflex docking and LigScore1 rescoring, SF: compounds after Surflex docking and postprocessing. Consensus: common compounds between SF/LS1 and SF among the top 3000 ranked molecules.

Asp, Glu, His, Cys, Tyr). Groups in the vicinity of the binding pocket showed normal titration behavior except for the catalytic C473 which was determined to be completely ionized at pH 7 in agreement with its known experimental pK_a value of 5.9.²⁶ The catalytic site of CDC25B is located next to a relatively large groove, the so-called inhibitor-binding pocket. Hence, we defined the binding site for our docking experiments as a combination of two binding pockets, the catalytic site (around C473) and the inhibitor-binding pocket.^{26,27}

Virtual Screening. The VLS experiments were performed applying a multistep hierarchical protocol using three in silico screening packages: FRED,²⁸ Surflex,²⁹ and LigandFit³⁰ (see Figure 1). We used the 2005 release of the ChemBridge database (429 623 compounds in 2D SDF format) which was first filtered using the programs FILTER (OpenEye Software Inc., Santa Fe, U.S.A., <http://www.eyesopen.com/>) and FAF-Drugs³¹ in order to remove nondruglike compounds and reactive/toxic groups (over 150 functional groups were assessed/tested including quinones). Second, the resulting library containing 313 569 druglike compounds was converted into 3D structures (up to 50 conformers per compound), and hydrogen atoms and Gasteiger partial charges were assigned with OMEGA (OpenEye Software Inc., Santa Fe, U.S.A.). The first docking step was carried out using the rigid body-docking program FRED. The top 50 000 compounds were then redocked and scored using the program Surflex. The postprocessing step was performed after investigation of the nature of the binding pocket (i.e., polar, hydrophobic, solvent exposed)³² and calibration of postprocessing parameters with some known CDC25 inhibitors (as performed in numerous studies, e.g., as in ref 33). In parallel, the program LigandFit and the LigScore1 scoring function were also used. One hundred steps of rigid-body minimization with the LigandFit minimizer were performed for each of the 50 000 docked ligands followed by a rescoring step with LigScore1.

Compounds Selection. Two distinct compound lists were created, the Surflex top ranked compounds after postpro-

cessing with nondefault parameters³² and the Ligand/LigScore1 top ranked compounds. We decided to select a list of 1500 compounds for experimental screening. First, we selected compounds present in both lists within the top 3000 best scored molecules (so-called consensus compounds). Six hundred compounds were present in both lists (Consensus list). In addition, 450 top scoring nonconsensus molecules after Surflex docking and scoring (SF list) and 450 top scoring nonconsensus compounds after Surflex docking, minimization by LigandFit, and rescoring with LigScore1 (SF/LS1 list) were selected.

In Vitro Enzymatic Assay. The assay was performed in 96-well plates in a final volume of 200 μ L. The maltose binding protein-CDC25B was kept in an elution buffer [50 mM phosphate pH 7.5, 300 mM NaCl, 500 mM imidazole, 10% glycerol]. It was diluted in an assay buffer [30 mM Tris-HCl (pH 8.2), 75 mM NaCl, 0.67 mM EDTA, 0.033% BSA, 1 mM DTT] such that the final concentration of CDC25B was 75 ng/well. The reaction was initiated by addition of 30 μ M of fluoresceine diphosphate followed by an immediate measure of fluoresceine monophosphate emission with a Fluoroskan Ascent (Lab Systems; excitation filter: 485 nm, emission filter: 530 nm). The selected 1500 compounds were studied at a concentration of 100 μ M. The results were expressed as the means of at least two independent experiments with three determinations per tested concentration and per experiment. For each compound, the drug concentration required for 50% inhibition (IC₅₀) was determined from a sigmoidal dose-response curve using GraphPad Prism (GraphPad Software, San Diego, CA). The NMR spectra of the 5 best molecules are shown as supplementary figures in the Supporting Information.

Clonogenic Assay. The most potent inhibitors (compounds 1 and 2) were also investigated on cell proliferation in a clonogenic assay. HeLa cells (Aptanomics, Lyon, France) were plated at a concentration of 100 cells/well in 6-well culture plates with 2.5 mL of medium/well. After 24 h growing at 37 °C in a humidified atmosphere of 5% CO₂, the culture medium was replaced by Dulbecco's minimal

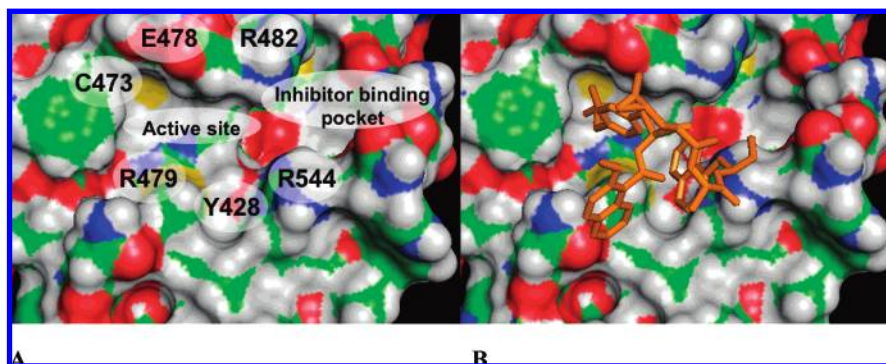


Figure 2. A. The catalytic site and inhibitor-binding pocket of CDC25B. B. The BASF experimental peptide structure transposed into the CDC25B 1CWT X-ray structure. The molecular surface of the protein is shown as a solid surface, in red, oxygen atoms; blue, nitrogen; green, carbon; and white, hydrogen atoms. The catalytic site and inhibitor-binding pocket are labeled for orientation. The peptide is shown in orange and interacts essentially with the catalytic site area but also has some contacts with the entrance of the inhibitor-binding pocket. The figures were generated with PyMol.

essential medium containing 10% fetal calf serum or medium containing inhibitors at increasing concentrations (from 0.05 μM to 60 μM) and incubated for 10 days. Cells were then washed with phosphate-buffered saline and fixed in 10% formaldehyde for 15 min at room temperature. They were carefully rinsed with water, stained with 1 mL of crystal violet (2 g in 100 mL of ethanol and then 2 mL in 100 mL of water) for 15 min, and finally rinsed with water. The plating efficiency was determined by counting the colonies. The results are expressed as the means of two independent experiments with three determinations per tested concentration and per experiment. For each compound, the drug concentration required for 50% inhibition was determined from a sigmoidal dose–response curve using GraphPad Prism (GraphPad Software, San Diego, CA).

RESULTS AND DISCUSSION

Selection of the CDC25B Experimental Structure and Definition of the Binding Pockets. The first nontrivial step for our SB-VLS experiment was the definition of the putative binding pocket. Indeed, structural analysis of this region in the context of previously reported experimental data was judged essential in order to better understand the critical structural features important for ligand/substrate binding. This step was in fact essential because docking experiments on CDC25 are notoriously difficult essentially due to the architecture of the binding region.^{34,35} The catalytic C473 is located at the bottom of a shallow active site pocket and next to a larger groove (Figure 2A), the so-called inhibitor-binding pocket. This latter displays several positively charged residues such as R544 and R482, expected to play a role in the binding of some but not all inhibitors.^{18,26,27,34} Twelve crystal structures of ligand-free CDC25B are available at the PDB, and, in addition, one CDC25B structure cocrystallized with a modified peptide that blocks the active site has been reported in a recent patent application by BASF (Figure 2B).³⁶ Among the CDC25B crystal structures present at the PDB, the best candidates for a docking study are 1CWT (resolution 2.3 Å),⁸ 1QB0 (resolution 1.91 Å),⁸ and 1YMK (apo form, resolution 1.7 Å),³⁷ while other structures can have the catalytic site pocket partially or fully inaccessible like when a disulfide bond is formed between the active site C473 and C426.³⁷ The 1CWT, 1QB0, BASF, and 1YMK experimental structures are highly similar with rmsd devia-

tions between backbone atoms ranging from 0.20 Å to 0.35 Å. However, in these structures and within the catalytic site-inhibitor-binding pocket region, the conformation of E478, R482, and R544 amino acid side chains differs. In all these experimental structures but BASF, the R544 side chain occludes one region of the inhibitor-binding pocket. In the BASF structure, the small peptide ligand contacts not only the catalytic pocket (C473) region but also the area of R544/Y428 (see Figure 2B)³⁶ and pushes the side chain of R544 away, opening this region of the inhibitor-binding pocket. As such, we decided to select the side-chain conformation seen in the BASF structure for residue R544 for our docking/scoring exercise. However, in the BASF structure, the side chains of E478 and R482 partially occlude another part of the inhibitor-binding pocket, while they have a more open conformation in 1CWT or 1QB0. We kept the orientation of these two side chains as present in the 1CWT or the 1QB0 structure for our docking experiments. In fine, we used the R544 side-chain reoriented 1CWT structure for our SB-VLS computations. Opening a binding pocket manually or through simulation to somewhat mimic an induced-fit effect can be used in docking experiments, as shown in ref 38, while the selection of an experimental structure based on the resolution does not apply in our case since the structures are nearly identical.

These two pockets (the catalytic site and the inhibitor-binding pocket) contain mobile water molecules as judged by their very high B-factor values. A bound sulfate (for example in the case of 1CWT) is also present in the catalytic site, next to C473, that should mimic the incoming phosphate group of the substrate. No water molecules were present in the BASF structure, but 8 water molecules have to be displaced upon peptide-binding as seen when transposing the peptide from the BASF structure to, for example, the 1CWT structure. Removal of these water molecules in the catalytic site area has been observed before, like when a phosphate group binds near the catalytic C473.³⁷ For the remaining 6 water molecules that could be present in the inhibitor-binding pocket even in the presence of the peptide, all of them have relatively high B-factor values. Therefore, given the lack of experimental structures of CDC25 cocrystallized with a small druglike ligand, we believe that, for the time being, there is no rationale in keeping water molecules during SB-VLS experiments for this protein. In fact, removing water

Table 1. Inhibitory Activity on CDC25B of the Best Compounds after SB-VLS

% inhibition at 100 μ M no. of compounds	21–40	41–50	51–60	61–90	91–100
	76	13	7	1	2

molecules when their contribution to binding is unknown is commonly performed in SB-VLS studies (see for instance refs 34 and 39).

In parallel with the above investigation, we analyzed theoretically the binding regions of CDC25 and predicted the most likely druggable area with the Pocket-Finder utility of the ICM package.⁴⁰ For this purpose, our modified unliganded 1CWT crystal structure was used. The most energetically favorable binding pocket encloses both the catalytic pocket and the inhibitor-binding pocket. These observations suggest that both areas, the catalytic site and the inhibitor-binding pocket, should be explored by the docking algorithms. This choice is also supported by a previously reported docking study which suggests that small CDC25 inhibitors could bind to the inhibitor-binding pocket and/or to the catalytic site, depending on their size and chemical structure.³⁴ These two pockets (catalytic site and inhibitor-binding pocket) together have a volume of about 455 Å³; such a site is geometrically fully compatible with what is known about pockets interacting with druglike compounds.⁴⁰

We thus applied on these two pockets our multistep docking protocol (Figure 1) as described in refs 32 and 41 since we⁴² and others⁴³ have been able to identify promising hits on difficult targets using this strategy. We decided to combine three in silico screening packages, FRED, Surflex, and LigandFit, since these tools have been shown to be effective in reproducing experimental ligand binding modes. We used a compound collection containing 313 569 druglike compounds. The first docking step was carried out using a rigid body-docking procedure (FRED) to generate a focused library containing molecules having an appropriate shape complementarity with the CDC25 binding pockets. The top 50 000 compounds were then redocked and scored using Surflex (fragment-based docking). One hundred steps of rigid-body minimization were performed with LigandFit for each of the 50 000 docked ligands followed by a rescoring step with the LigScore1 scoring function. The final compound selection was performed after Surflex postprocessing, LigScore1 ranking, and visual inspection.

Hit Validation and Experimental Testing. Among the 1500 compounds selected in silico, 99 molecules showed at least 20% inhibitory activity on CDC25B at a concentration of 100 μ M (6.6% of the 1500 selected compounds, see Table 1). Eleven compounds were found to inhibit the enzymatic activity of CDC25B by more than 50% at the same concentration (Table 2). The most potent molecules, compounds 1 and 2 (Table 2), inhibited CDC25B with IC₅₀ values of 13 and 19 μ M, respectively. These two molecules are among the most potent nonquinonic derivative inhibitors reported to date for this protein. Moreover, compounds 1 and 2 also display antiproliferative properties. Indeed, they are effective at inhibiting clonal proliferation of HeLa cells in a concentration dependent-manner with IC₅₀ values of 15.8 and 3.6 μ M, respectively. We have not yet established that these compounds inhibit only CDC25 within the cells; this will require additional investigations.

From a chemical standpoint, compounds 1 and 5 belong to the same class sharing a thiazolopyrimidinone core, while compounds 2 and 5 possess the common feature 5-(4-carboxyphenyl)furyl linked to two different bicyclic moieties.

It is interesting to note that compound 1 was identified only by applying a consensus approach. Compound 1 was ranked 1602 with Surflex, while it was found at position 2493 with Ligscore1 (Table 2). Thus, without applying a consensus approach, it would not have been possible to identify this molecule when testing a hit list of 1500 molecules. However, Surflex identified most of the active compounds (e.g., compounds 2, 4, and 5). Very few of the most active compounds had “good” ranks after LigScore1 rescoring. Yet, we found some “hits” at 100 μ M with LigScore1 (e.g., compounds 7, 8, and 9 ranked respectively 57, 420, and 596).

Predicted Binding Mode. To understand the enzymatic inhibition mechanism of CDC25B, Lavecchia et al.³⁴ recently proposed docking models of six representative CDC25 inhibitors (thus essentially quinone derivatives). In that study, the authors docked known actives with AutoDock and Gold and validated the predicted binding poses in light of available structure–activity and site directed mutagenesis data. Although the binding mode of the docked ligands is not fully confirmed with several alternative orientations for all compounds, the main conclusion from that study is that the ligands seem to contact both the active site and the inhibitor-binding pocket as well as the connection area in between these two cavities (area of residue Y428) (Figure 2A). We performed additional computational docking studies on compound 1 with Surflex and LigandFit and generated consensus docking poses. Compound 1 was docked again with both packages, and 20 poses were saved and compared in terms of rmsd and predicted binding energy. Among the top-ranked binding modes, two main poses for compound 1 were found to be nearly identical when comparing the orientations proposed by Surflex and LigandFit. Although our compound is structurally different from previously reported ones, our two predicted binding modes (Figure 3) seem to be in good agreement with the overall positioning of CDC25B inhibitors proposed by Lavecchia et al.³⁴ When comparing Figures 2B and 3, some similarities between the cocrystallized peptide and compound 1 can be noticed. First, we note that for both binding models of compound 1, the thiazolopyrimidine core is placed at the junction between the two binding pockets, next to the CDC25 Y428 side chain (Figure 3), while the hydroxyphenyl moiety is located in the inhibitor-binding pocket. In one binding model (pose 1), the phenyldioxolane moiety stacks against the R544 side chain (Figure 3, top), while in the other predicted complex (pose 2), this ring system is located in the catalytic pocket (Figure 3, bottom). When comparing our predicted binding pose for compound 1 with the BASF crystal of CDC25B in the complex with a modified peptide, we observe that most of our compound mimics well the binding mode of either the beta-(2-naphthyl)alanine of the peptide (Figure 2B and Figure 3, pose 1) or the sulfonated tyrosine (Figure 2B and Figure 3, pose 2), while many of the remaining atoms of compound 1 follow the overall orientation of the peptide (please see supplement Figure 2 in the Supporting Information). In pose 1, compound 1 is predicted to make a total of 3 hydrogen bonds, two with the side chain of R482 and one with the

Table 2. CDC25B in Silico and Experimental Data^a

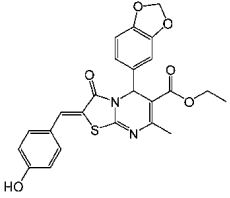
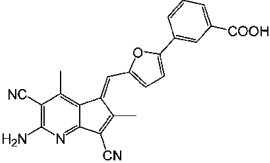
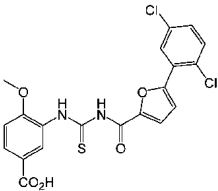
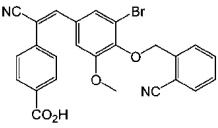
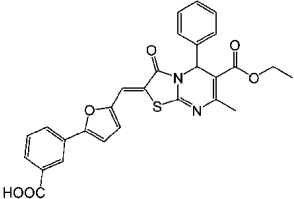
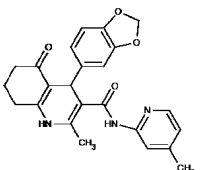
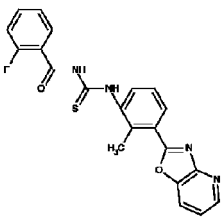
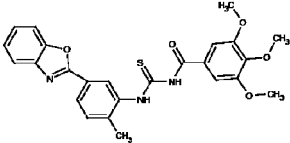
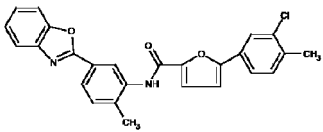
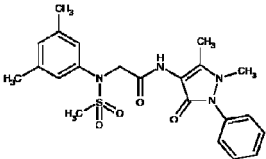
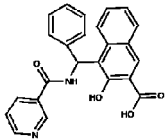
Compound	Surflex Ranking (score value)	LigScore1 ranking (score value)	% Inhibition CDC25B activity at 100 μ M	IC ₅₀ (μ M) MBP- CDC25B	IC ₅₀ (μ M) HeLa clonogenic assay
1 	1602 (6.48)	2493 (5.20)	98	13.0\pm0.5	15.8 \pm 1.8
2 	50 (8.64)	2221 (5.26)	94	19.0\pm1.3	3.6 \pm 1.2
3 	1085 (6.73)	1582 (5.40)	58	84\pm9	n.d.
4 	341 (7.47)	5288 (4.81)	48	80\pm8.7	n.d.
5 	59 (8.46)	1695 (5.37)	63	74.6\pm3.6	n.d.
6 	686 (7.03)	2826 (5.15)	52	n.d.	n.d.

Table 2 (Continued)

<p>7</p> 	2348 (6.20)	57 (6.34)	58	n.d.	n.d.
<p>8</p> 	1452 (6.54)	420 (5.84)	51	n.d.	n.d.
<p>9</p> 	2347 (6.20)	596 (5.75)	56	n.d.	n.d.
<p>10</p> 	1133 (6.70)	1314 (5.47)	52	n.d.	n.d.
<p>11</p> 	1270 (6.63)	2931 (5.13)	51	n.d.	n.d.

^a Surflex and LigandFit-Ligscore1 rankings, score values, inhibitory activities, and IC₅₀ values for the most active compounds on CDC25B in vitro and IC₅₀ values of the most active compounds on HeLa cells clonogenic activity. n.d. not determined.

side chain of R544. In addition, several hydrophobic contacts are noticed. In pose 2, compound 1 is predicted to make a total of 4–6 hydrogen bonds with the side chains of R479, Y428, R482, and E446 and the backbone NH atoms of R479, E474, and possibly E478. In order to investigate further the binding mode of compound 1, we initiated site directed mutagenesis experiments. The preliminary results suggest that R544 does not play a critical role in the binding of compound 1 since its mutation to Q did not modify significantly the affinity (IC₅₀ = 13 μ M for the wild-type and IC₅₀ = 18.6 μ M for the R544Q mutant). Another mutant CDC25 molecule was generated with a Y428A substitution.

Structurally, such substitution should enlarge the binding pocket at the level of the catalytic site-inhibitor binding pocket junction and could either perturb binding or enhance affinity. The inhibitory activity of compound 1 with the mutant Y428A (IC₅₀ = 1.6 μ M for the mutant compared to IC₅₀ = 13 μ M for the wild-type) analyzed in the context of the CDC25 crystal structure and of results reported by Lavecchia et al.³⁴ suggests that this region of the protein is in direct contact with the inhibitor. We propose that reducing the size of the Tyr side chain (mutant Y428A) would allow the compound to insert deeper into the inhibitor binding pocket, thereby improving the overall affinity (i.e., gain of

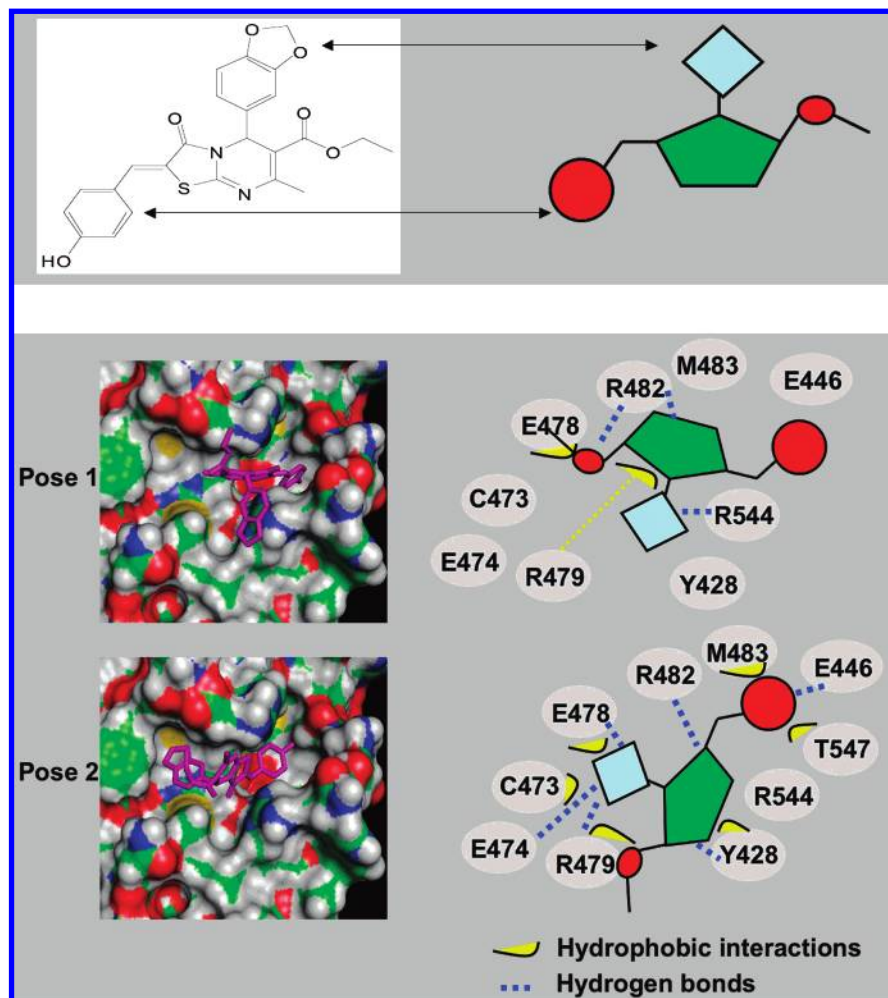


Figure 3. Proposed binding modes for compound 1. Two main binding modes generated by Surflex and LigandFit for compound 1 (shown in magenta) are shown (left). The figure was generated with PyMol. To the right, a 2D projection map of these two poses showing some key interactions between the ligand and the protein is presented. A schematic representation of the compound is used to simplify the reading of the figure. Pose 1: the phenyldioxolane moiety of compound 1 is next to R544. Pose 2: the phenyldioxolane moiety of compound 1 is inside the catalytic pocket.

function mutant). The Y428A mutation should not damage the overall nor the local structure of CDC25 since compound 1 appears to fit better in the binding pocket. Taking these results and observations together, we suggest that the most likely binding mode for compound 1 should resemble pose 2. Further experiments such as X-ray crystallography are however needed to fully confirm this hypothesis.

Hit Rate. The present hit rate is relatively low (0.3%) but should be analyzed in the context of our main objective (i.e., find CDC25B inhibitors with a new scaffold and not quinone-like). Generally HTS hit rates range from 0.02 to 0.05%^{39,44} but can also give better results, as shown after screening CDC25 with a 10 070 compound collection⁴⁵ (the hit rate was 0.20%, most compounds belonged to the quinone family). In SB-VLS studies, hit rates can be between 1 and 5% or higher (see for example ref 46). However, in such cases, several key pieces of information are usually supplied, including, for example, a pharmacophore model and known compounds cocrystallized in the binding pocket to calibrate the scoring functions and validate the pose. In our study, we did not want to use ligand-based approaches as the goal was to escape as much as possible from the known scaffolds. The protocol and the docking/scoring engines used have been shown to be efficient,^{32,41–43,47} but it is also important to keep

in mind that SB-VLS methods do not perform consistently well on all targets.⁴⁸ This might be the situation in the present study, but we believe that the relatively low hit rate comes from the fact that the CDC25 binding pocket is very difficult to screen (i.e., flexible side chains, water molecules have to be displaced). Further in silico experiments on CDC25 would be needed in order to see if a better hit rate could be obtained, like with algorithms that can handle local structural changes during docking⁴⁹ or methods that are expected to evaluate accurately the overall dynamics and energetics of a system (e.g., MD-PB-(or GB)-SA).⁵⁰

In conclusion, SB-VLS/in vitro experiments have been used to discover novel low molecular weight inhibitors of CDC25B. About 100 molecules with significant inhibition were identified. Among those are two good candidates for further optimization as they feature a potent CDC25B inhibition in vitro and have antiproliferative effects. Both compounds have affinity values similar to the best inhibitors of CDC25B but are structurally different from the existing CDC25 ligands and should not be reactive. A likely binding mode of the most potent compound is proposed. Our data should help in future structure–function studies on CDC25 and could, after optimization, facilitate the design of novel anticancer drugs.

ACKNOWLEDGMENT

Financial support from the “Ligue Nationale Contre le Cancer” and INSERM is greatly appreciated. We thank BASF for providing the PDB file of the CDC25B-peptide complex.

Supporting Information Available: NMR spectra for the 5 best inhibitors of CDC25 identified in our study (supplement Figure 1) and proposed binding modes for compound 1 superimposed onto the BASF peptide-inhibitor (supplement Figure 2). This material is available free of charge via the Internet at <http://pubs.acs.org>.

REFERENCES AND NOTES

- Nilsson, I.; Hoffmann, I. Cell cycle regulation by the Cdc25 phosphatase family. *Prog. Cell Cycle Res.* **2000**, *4*, 107–14.
- Boutros, R.; Dozier, C.; Ducommun, B. The when and wheres of CDC25 phosphatases. *Curr. Opin. Cell Biol.* **2006**, *18* (2), 185–91.
- Galaktionov, K.; Beach, D. Specific activation of cdc25 tyrosine phosphatases by B-type cyclins: evidence for multiple roles of mitotic cyclins. *Cell* **1991**, *67* (6), 1181–94.
- Nagata, A.; Igarashi, M.; Jinno, S.; Suto, K.; Okayama, H. An additional homolog of the fission yeast cdc25+ gene occurs in humans and is highly expressed in some cancer cells. *New Biol.* **1991**, *3* (10), 959–68.
- Sadhu, K.; Reed, S. I.; Richardson, H.; Russell, P. Human homolog of fission yeast cdc25 mitotic inducer is predominantly expressed in G2. *Proc. Natl. Acad. Sci. U.S.A.* **1990**, *87* (13), 5139–43.
- Karlsson, C.; Katich, S.; Hagting, A.; Hoffmann, I.; Pines, J. Cdc25B and Cdc25C differ markedly in their properties as initiators of mitosis. *J. Cell Biol.* **1999**, *146* (3), 573–84.
- Fauman, E. B.; Cogswell, J. P.; Lovejoy, B.; Rocque, W. J.; Holmes, W.; Montana, V. G.; Piwnicka-Worms, H.; Rink, M. J.; Saper, M. A. Crystal structure of the catalytic domain of the human cell cycle control phosphatase, Cdc25A. *Cell* **1998**, *93* (4), 617–25.
- Reynolds, R. A.; Yem, A. W.; Wolfe, C. L.; Deibel, M. R., Jr.; Chidester, C. G.; Watenpaugh, K. D. Crystal structure of the catalytic subunit of Cdc25B required for G2/M phase transition of the cell cycle. *J. Mol. Biol.* **1999**, *293* (3), 559–68.
- Galaktionov, K.; Lee, A. K.; Eckstein, J.; Draetta, G.; Meckler, J.; Loda, M.; Beach, D. CDC25 phosphatases as potential human oncogenes. *Science* **1995**, *269* (5230), 1575–7.
- Takemasa, I.; Yamamoto, H.; Sekimoto, M.; Ohue, M.; Noura, S.; Miyake, Y.; Matsumoto, T.; Aihara, T.; Tomita, N.; Tamaki, Y.; Sakita, I.; Kikkawa, N.; Matsuura, N.; Shiozaki, H.; Monden, M. Overexpression of CDC25B phosphatase as a novel marker of poor prognosis of human colorectal carcinoma. *Cancer Res.* **2000**, *60* (11), 3043–50.
- Gasparotto, D.; Maestro, R.; Piccinin, S.; Vukosavljevic, T.; Barzan, L.; Sulfaro, S.; Boiocchi, M. Overexpression of CDC25A and CDC25B in head and neck cancers. *Cancer Res.* **1997**, *57* (12), 2366–8.
- Wu, W.; Fan, Y. H.; Kemp, B. L.; Walsh, G.; Mao, L. Overexpression of cdc25A and cdc25B is frequent in primary non-small cell lung cancer but is not associated with overexpression of c-myc. *Cancer Res.* **1998**, *58* (18), 4082–5.
- Boutros, R.; Lobjois, V.; Ducommun, B. CDC25 Phosphatases in cancer cells: key players ? good targets ? *Nat. Rev. Cancer* **2007**, in press.
- Kristjansdottir, K.; Rudolph, J. Cdc25 phosphatases and cancer. *Chem. Biol.* **2004**, *11* (8), 1043–51.
- Lyon, M. A.; Ducruet, A. P.; Wipf, P.; Lazo, J. S. Dual-specificity phosphatases as targets for antineoplastic agents. *Nat. Rev. Drug Discovery* **2002**, *1* (12), 961–76.
- Prevost, G. P.; Brezak, M. C.; Goubin, F.; Mondesert, O.; Galcera, M. O.; Quaranta, M.; Alby, F.; Lavergne, O.; Ducommun, B. Inhibitors of the CDC25 phosphatases. *Prog. Cell Cycle Res.* **2003**, *5*, 225–34.
- Brisson, M.; Nguyen, T.; Vogt, A.; Yalowich, J.; Giorgianni, A.; Tobi, D.; Bahar, I.; Stephenson, C. R.; Wipf, P.; Lazo, J. S. Discovery and characterization of novel small molecule inhibitors of human Cdc25B dual specificity phosphatase. *Mol. Pharmacol.* **2004**, *66* (4), 824–33.
- Contour-Galcera, M. O.; Sidhu, A.; Prevost, G.; Bigg, D.; Ducommun, B. What's new on CDC25 phosphatase inhibitors. *Pharmacol. Ther.* **2007**, *115* (1), 1–12.
- Lazo, J. S.; Aslan, D. C.; Southwick, E. C.; Cooley, K. A.; Ducruet, A. P.; Joo, B.; Vogt, A.; Wipf, P. Discovery and biological evaluation of a new family of potent inhibitors of the dual specificity protein phosphatase Cdc25. *J. Med. Chem.* **2001**, *44* (24), 4042–9.
- Brezak, M. C.; Quaranta, M.; Contour-Galcera, M. O.; Lavergne, O.; Mondesert, O.; Auvray, P.; Kasprzyk, P. G.; Prevost, G. P.; Ducommun, B. Inhibition of human tumor cell growth in vivo by an orally bioavailable inhibitor of CDC25 phosphatases. *Mol. Cancer Ther.* **2005**, *4* (9), 1378–87.
- Kitchen, D. B.; Decornez, H.; Furr, J. R.; Bajorath, J. Docking and scoring in virtual screening for drug discovery: methods and applications. *Nat. Rev. Drug Discovery* **2004**, *3* (11), 935–49.
- Shoichet, B. K. Virtual screening of chemical libraries. *Nature* **2004**, *432* (7019), 862–5.
- Berman, H. M.; Westbrook, J.; Feng, Z.; Gilliland, G.; Bhat, T. N.; Weissig, H.; Shindyalov, I. N.; Bourne, P. E. The Protein Data Bank. *Nucleic Acids Res.* **2000**, *28* (1), 235–42.
- Bashford, D.; Karplus, M. pKa's of ionizable groups in proteins: atomic detail from a continuum electrostatic model. *Biochemistry* **1990**, *29* (44), 10219–25.
- Miteva, M. A.; Tuffery, P.; Villoutreix, B. O. PCE: web tools to compute protein continuum electrostatics. *Nucleic Acids Res.* **2005**, *33*, Web Server issue, W372–5.
- Chen, W.; Wilborn, M.; Rudolph, J. Dual-specific Cdc25B phosphatase: in search of the catalytic acid. *Biochemistry* **2000**, *39* (35), 10781–9.
- Rudolph, J. Catalytic mechanism of Cdc25. *Biochemistry* **2002**, *41* (49), 14613–23.
- McGann, M. R.; Almond, H. R.; Nicholls, A.; Grant, J. A.; Brown, F. K. Gaussian docking functions. *Biopolymers* **2003**, *68* (1), 76–90.
- Jain, A. N. Surflex: fully automatic flexible molecular docking using a molecular similarity-based search engine. *J. Med. Chem.* **2003**, *46* (4), 499–511.
- Venkatachalam, C. M.; Jiang, X.; Oldfield, T.; Waldman, M. LigandFit: a novel method for the shape-directed rapid docking of ligands to protein active sites. *J. Mol. Graphics Modell.* **2003**, *21* (4), 289–307.
- Miteva, M. A.; Violas, S.; Montes, M.; Gomez, D.; Tuffery, P.; Villoutreix, B. O. FAF-Drugs: Free ADME/tox Filtering of compound collections. *Nucleic Acids Res.* **2006**, *34*, W738–744.
- Miteva, M. A.; Lee, W. H.; Montes, M. O.; Villoutreix, B. O. Fast structure-based virtual ligand screening combining FRED, DOCK, and Surflex. *J. Med. Chem.* **2005**, *48* (19), 6012–22.
- Cavasotto, C. N.; Ortiz, M. A.; Abagyan, R. A.; Piedrafita, F. J. In silico identification of novel EGFR inhibitors with antiproliferative activity against cancer cells. *Bioorg. Med. Chem. Lett.* **2006**, *16* (7), 1969–74.
- Lavecchia, A.; Cosconati, S.; Limongelli, V.; Novellino, E. Modeling of Cdc25B dual specificity protein phosphatase inhibitors: docking of ligands and enzymatic inhibition mechanism. *ChemMedChem* **2006**, *1* (5), 540–50.
- Rudolph, J. Cdc25 phosphatases: structure, specificity, and mechanism. *Biochemistry* **2007**, *46* (12), 3595–604.
- Taylor, N. R.; Borhani, D.; Epstein, D.; Rudolph, J.; Ritter, K.; Fujimori, T.; Robinson, S.; Eckstein, J.; Haupt, A.; Walker, N.; Dixon, R.; Choquette, D.; Blanchard, J.; Kluge, A.; Pal, K.; Bockovich, N.; Come, J.; Hediger, M. WO; BASF AG, Germany; GPC Biotech Inc., U.S.A.; 2001; 01/16300A2.
- Buhrman, G.; Parker, B.; Sohn, J.; Rudolph, J.; Mattos, C. Structural mechanism of oxidative regulation of the phosphatase Cdc25B via an intramolecular disulfide bond. *Biochemistry* **2005**, *44* (14), 5307–16.
- Huang, N.; Kalyanaraman, C.; Bernacki, K.; Jacobson, M. P. Molecular mechanics methods for predicting protein-ligand binding. *Phys. Chem. Chem. Phys.* **2006**, *8* (44), 5166–77.
- Jenkins, J. L.; Kao, R. Y.; Shapiro, R. Virtual screening to enrich hit lists from high-throughput screening: a case study on small-molecule inhibitors of angiogenin. *Proteins* **2003**, *50* (1), 81–93.
- An, J.; Totrov, M.; Abagyan, R. Comprehensive identification of “druggable” protein ligand binding sites. *Genome Inform. Ser. Workshop Genome Inform.* **2004**, *15* (2), 31–41.
- Montes, M.; Miteva, M. A.; Villoutreix, B. O. Structure-based virtual ligand screening with LigandFit: pose prediction and enrichment of compound collections. *Proteins* **2007**, *68*, 712–25.
- Segers, K.; Sperandio, O.; Sack, M.; Fischer, R.; Miteva, M. A.; Rosing, J.; Nicolaes, G. A. F.; Villoutreix, B. O. Design of protein–membrane interaction inhibitors by virtual ligand screening, proof of concept with the C2 domain of factor V. *Proc. Natl. Acad. Sci. U.S.A.* **2007**, *31*, 12697–12702.
- Cozza, G.; Bonvini, P.; Zorzi, E.; Poletto, G.; Pagano, M. A.; Sarno, S.; Donella-Deana, A.; Zagotto, G.; Rosolen, A.; Pinna, L. A.; Meggio, F.; Moro, S. Identification of ellagic acid as potent inhibitor of protein

- kinase CK2: a successful example of a virtual screening application. *J. Med. Chem.* **2006**, *49* (8), 2363–6.
- (44) Zolli-Juran, M.; Cechetto, J. D.; Hartlen, R.; Daigle, D. M.; Brown, E. D. High throughput screening identifies novel inhibitors of *Escherichia coli* dihydrofolate reductase that are competitive with dihydrofolate. *Bioorg. Med. Chem. Lett.* **2003**, *13* (15), 2493–6.
- (45) Lazo, J. S.; Nemoto, K.; Pestell, K. E.; Cooley, K.; Southwick, E. C.; Mitchell, D. A.; Furey, W.; Gussio, R.; Zaharevitz, D. W.; Joo, B.; Wipf, P. Identification of a potent and selective pharmacophore for Cdc25 dual specificity phosphatase inhibitors. *Mol. Pharmacol.* **2002**, *61* (4), 720–8.
- (46) Lu, Y.; Nikolovska-Coleska, Z.; Fang, X.; Gao, W.; Shangary, S.; Qiu, S.; Qin, D.; Wang, S. Discovery of a nanomolar inhibitor of the human murine double minute 2 (MDM2)-p53 interaction through an integrated, virtual database screening strategy. *J. Med. Chem.* **2006**, *49* (13), 3759–62.
- (47) Kellenberger, E.; Rodrigo, J.; Muller, P.; Rognan, D. Comparative evaluation of eight docking tools for docking and virtual screening accuracy. *Proteins* **2004**, *57* (2), 225–42.
- (48) Krovat, E. M.; Steindl, T.; Langer, T. Recent Advances in Docking and Scoring. *Curr. Comput.-Aided Drug Des.* **2005**, *1*, 1.
- (49) Zentgraf, M.; Steuber, H.; Koch, C.; La Motta, C.; Sartini, S.; Sotriffer, C. A.; Klebe, G. How reliable are current docking approaches for structure-based drug design? Lessons from aldose reductase. *Angew. Chem., Int. Ed.* **2007**, *46* (19), 3575–8.
- (50) Huang, N.; Kalyanaraman, C.; Irwin, J. J.; Jacobson, M. P. Physics-based scoring of protein-ligand complexes: enrichment of known inhibitors in large-scale virtual screening. *J. Chem. Inf. Model.* **2006**, *46* (1), 243–53.

CI700313E